Journal of Molecular Liquids xxx (xxxx) xxx

Contents lists available at ScienceDirect

Journal of Molecular Liquids

journal homepage: www.elsevier.com/locate/molliq

Effect of internal charge distribution on the electrophoretic mobility of poly(N-isopropylacrylamide) based core-shell microgel particles

Imre Varga [a,b,*], Attila Kardos [a,b], Attila Borsos [a], Tibor Gilányi [a]

[a] Institute of Chemistry, Eötvös Loránd University, H-1117, Budapest, P.O. Box 32, Hungary
[b] Department of Chemistry, University J. Selyeho, 945 01, Komarno, Slovakia

ARTICLE INFO

Article history:
Received 8 October 2019
Received in revised form 17 October 2019
Accepted 19 October 2019
Available online xxxx

Keywords:
Intelligent microgel
Electrophoretic mobility
pNIPAm
Draining model
Non-draining model

ABSTRACT

The electrophoretic mobility of poly(*N*-isopropylacrylamide) and poly(*N*-isopropylacrylamide-co-acrylic acid) copolymer particles, as well as different core-shell microgel particles (neutral core with charged shell and charged core with neutral shell) was investigated as function of microgel swelling. The swelling of the microgels were varied with increasing the temperature. To interpret the experimental results, we used scaling arguments to show that due to the strong hydrodynamic interactions the inner part of the microgel particles are non-draining in low ionic strength media and only the outmost thin shell of the microgel contributes actively to the electrophoretic mobility. We found that the experimental results were in good agreement with the prediction of this model, while we found physical inconsistencies when the experiments were analysed in terms of the draining models often used in the literature.

1. Introduction

In recent years, considerable interest has been focused on the development of "smart" aqueous microgels whose properties change dramatically upon the application of a specific environmental stimulus (e.g. temperature change). While a variety of polymer systems have been explored, most attention has been payed to microgels that are based on poly(N-isopropylacrylamide), pNIPAm [1]. Despite the fact that the charge distribution within the microgel particles has a profound effect on their properties (e.g. swelling and colloid stability) the possibilities for the characterization of the electrical structure of the microgel particles is rather limited. The total charge of the particles can be measured either by conductometric or potentiometric titration [2]. However, these measurements may only provide limited information on the charge distribution within the particle. Another widely used method to characterize the electrical properties of the microgel particles is to measure their electrophoretic mobility. These data provide crucial information to understand the colloid stability of these systems. However, if we are interested in the relationship between the mobility and the charge distribution within the soft gel particles the available literature seems rather ambiguous. Two concepts have been used to interpret the experimental mobility data of the microgel particles. Either the gel beads are treated as non-draining hard sphere colloids [3] or as spherically symmetric, draining polyelectrolytes [4] that are permeable to the solvent and mobile charged species. In the former case the electrophoretic mobility is determined by the electrokinetic charge (charges localized at the surface of the particle; i.e., the amount of charges, which are compensated beyond the slipping plane of the moving particle in the diffuse electric layer). However, in the latter case all fixed charges embedded into the gel network contribute to the mobility of the gel beads (for further details see below).

In the very first paper that investigated the temperature dependence of the electrophoretic mobility of pNIPAm microgel particles, Pelton et al. [3] have already used both a polyelectrolyte and a colloid particle model to fit the experimental mobility data. They concluded that though the surface charge model required 20 times less charge in a particle, the two fitted theoretical models resulted in rather similar curves that were in reasonable agreement with the experimental data.

Ohshima et al. [5] studied the electrophoretic mobility of polystyrene particles covered by a pNIPAm shell as a function of the ionic strength. They concluded that the draining model well describes the mobility below and above the LCST temperature of pNIPAm. However, it should be noted that when pNIPAm is in its collapsed state its water content reduces below 50% [6], thus it is rather questionable if the medium can indeed drain through the collapsed gel particle under these circumstances. Later, an extensive study was performed by Pichot

Abbreviations: NIPAm, *N*-isopropylacrylamide; BA, *N,N′*-methylenebis(acrylamide); AAc, acrylic acid; pNIPAm, poly(*N*-isopropylacrylamide); p(NIPAm-co-AAc), poly(*N*-isopropylacrylamide-co-acrylic acid); SDBS, sodium dodecylbenzenesulfonate; mM, mmol/dm^3 or mmol/L; M, mol/dm^3 or mol/L; *LCST*, Lower Critical Solution Temperature.

* Corresponding author. Laboratory of Interfaces and Nanosized Systems, Institute of Chemistry, Eötvös Loránd University, H-1117, Budapest, Pázmány Péter sétány 1/A, Hungary.
E-mail address: imo@chem.elte.hu (I. Varga).

https://doi.org/10.1016/j.molliq.2019.111979

et al. [7] on the electrophoretic mobility of latex particles composed of a polystyrene core and a pNIPAm or poly(NIPAm-co-aminoethyl methacrylate) shell. They measured the mobility of the latex particles as a function of pH, temperature and ionic strength. They concluded that the uniform polyelectrolyte layer model proposed by Ohshima could not describe their experimental data at low ionic strength but it worked at high salinity. They attributed this discrepancy to ionic strength induced charge distribution changes within the latex particles.

Fernandes et al. has investigated the electrophoretic mobility of ionic microgel particles (2-vinylpyridine crosslinked with divinylbenzene) as a function of pH in 1 mM NaCl [8]. They used Ohshima's theory for polyelectrolyte coated spherical particles [4] to model the experimental mobility data. As they highlighted in this paper the main challenge in the application of the draining polyelectrolyte models is that the hydrodynamic friction of the polyelectrolyte network usually cannot be calculated as the sum of the independent Stokes friction of the polyelectrolyte segments. To overcome this difficulty, they used an empirical function to describe the friction coefficient with changing polymer volume fraction in the gel particle. Finally, they concluded that the model can provide a qualitative description of the experimental data but quantitative fitting would require further refinements. In a next paper they also investigated the electrophoretic mobility of the same microgel particles as a function of the ionic strength both in the swollen and the collapsed state [9]. They arrived to the conclusion that the microgels behave as free-draining spherical polyelectrolytes in their swollen state and as charged hard spheres when they are collapsed.

Hoare et al. went one step further and investigated the electrophoretic mobility of microgel particles having identical overall charge but different internal charge distributions. Namely, they prepared carboxylic group containing microgel particles where the charges resided at or near the microgel surface (methacrylic acid/pNIPAm copolymer microgel) as well as microgels that incorporated more than one third of the carboxylic groups inside the gel beads (hydrolyzed acrylamide/pNIPAm copolymer microgels). They measured the mobility of the microgel particles in 1 mM KCl as a function of pH [2]. The most interestingly they found that in a pH range where carboxylic groups got charged in the core of the gel particles only particle swelling occurred, but significant mobility change could not be detected. At the same time when the charges are localized at the particle surface both particle swelling and increasing electrophoretic mobility can be observed in the relevant pH range. These results imply that only the surface charges contribute to the electrophoretic mobility of the gel particles. It should also be mentioned that similar results were found when the binding of an ionic surfactant (sodium dodecyl sulfate) was investigated to pNIPAm microgels. In that case the electrophoretic mobility of the gel beads also showed changes only when the surfactant binding was going on into the loosely crosslinked outer shell of the microgels [10]. Later Hoare at al. extended their investigation to an even wider range of microgel particles by using comonomers that accumulated in the shell of the microgels (vinylacetic acid and acrylic acid). They investigated the electrophoretic mobility of the non-functionalized pNIPAm and all four types of carboxylic acid functionalized microgels as a function of ionic strength and temperature [11]. Remarkably they observed non-zero plateau mobility values as a function of increasing ionic strength even for the non-functionalized pNIPAm in the fully collapsed state of the microgel particles. Based on these results they concluded that the pNIPAm-based microgel particles behave as soft (draining) particles even well above their collapse temperature. Based on this result they used Ohshima's model to acquire morphological information about the gel particles.

As it is shown by the above summary the literature results are rather contradicting in the question if the microgel beads behave as draining or non-draining particles during electrophoretic mobility measurements. The main difficulty in testing these models is that as it has been highlighted by Pelton [1,3] if suitable fitting parameters are chosen than both models can reproduce the experimental mobility values of the microgel particles. The motivation of our work was to gain further insight how the charges incorporated into the microgel particles contribute to the electrophoretic mobility of the gel beads and to test if either of the draining or the surface charge model could provide a physically consistent description of the experimental data. To achieve this goal, we prepared a pool of pNIPAm-based microgel particles with different but well-defined charge distributions: 'uncharged' pNIPAm particles, 'uniformly charged' pNIPAm-co-10%AAc particles and core-shell particles with either uncharged pNIPAm core and charged pNIPAm-co-10%AAc shell or charged pNIPAm-co-10%AAc core and 'uncharged' pNIPAm shell were prepared. We measured the electrophoretic mobility and hydrodynamic size of these microgel particles as a function of temperature. Finally, instead of fitting the mobility values using the charge density and the electrophoretic softness as free fitting parameters, an invariant quantity, the 'electrokinetic charge' of the microgel particles was calculated from experimental data and the variation of the particle softness was determined as a function of microgel swelling. Furthermore, based on recent literature results [12,13] we present scaling arguments that imply that only the charges present in a thin draining shell of the microgel contribute actively to the electrophoretic mobility while the inner part of the gel beads acts as a neutral hard sphere. We show that the experimental data are in good agreement with this physical picture.

2. Materials and methods

2.1. Materials

N-isopropylacrylamide (NIPAm, 99%) was purchased from Acros Organics and was recrystallized from hexane. *N,N′*-methylenebis(acrylamide) (BA, 99+%) was purchased from Alfa Aesar and was recrystallized from methanol. Acrylic acid (AAc, 99%, anhydrous) was obtained from Sigma-Aldrich and was distillated twice prior use. Sodium dodecylbenzenesulfonate (SDBS, technical grade) was purchased from Sigma-Aldrich and was used as received. Ammonium persulfate (APS, ACS Grade) was purchased from Amresco VWR and was used as received. All solutions were prepared in ultrapure MQ Water (Total Organic Content ≤ 5 ppb, Resistivity ≥ 18 MΩcm).

2.2. Synthesis of uniform microgels

The synthesis of the uniform microgel particles was based on the free-radical, precipitation polymerization method developed by Wu et al. [14] for the preparation of monodisperse pNIPAm microgel particles. The exact description of the synthesis procedure could be found in a previous article by Kardos et al. [15] The polymerization reaction was taken place in a double-walled reaction vessel which was connected to a high precision thermostat. The inert atmosphere was ensured by nitrogen. First, 250 mL of filtered Milli-Q water was filled into the reaction vessel and was purged for an hour at 80 °C. After an hour 74 mL of purged water was taken out from the reaction vessel and was stored under nitrogen until use. Calculated amount of NIPAm (3,14 g) and BA (142 mg) monomers were measured into a vial and was purged with nitrogen for 15 min before it was dissolved in 11 mL of oxygen-free water. APS (0.28 g/10 mL) and SDBS (0.46 g/10 mL) stock solutions were prepared in the same manner. All the stock solutions were stored under nitrogen until use. First, calculated amount of monomer stock solution (10 mL) was added into the reactor and was additionally purged for 30 min. This was followed by the addition of calculated amount of SDBS stock solution (2 mL) into the reaction vessel. The reaction mixture was additionally purged for 10 min. The reaction was started by the addition of calculated amount (2 mL) of APS stock solution. The reaction mixture was stirred by a magnetic stirrer at 1500 rpm for the first 30 s after the initiation. Later the stirring speed was decreased to 500 rpm. The reaction was continued for 4 h. The reaction was quenched by fast cooling and bubbling air through the

Please cite this article as: I. Varga, A. Kardos, A. Borsos, et al., Effect of internal charge distribution on the electrophoretic mobility of poly(N-isopropylacrylamide..., Journal of Molecular Liquids, https://doi.org/10.1016/j.molliq.2019.111979

reaction mixture. The pNIPAm latex mixture was purified from unreacted monomers and surfactant by extensive dialysis against Milli-Q water for 4 weeks giving supernatant conductivity of less than 5 μS/cm.

The above protocol was also used to prepare pNIPAm-co-10%AAc copolymer latex particles but in this case, 10 mol% of the NIPAm monomer was replaced by acrylic acid.

2.3. Preparation of core-shell microgel particles

To prepare pNIPAm core/pNIPAm-co-10%AAc shell as well as pNIPAm-co-10%AAc core/pNIPAm shell microgel particles a semi-batch precipitation polymerization method was used. The method is based on the semi-batch approach described by Antoniuk et al. [16] and Kardos et al. [17], recently. Namely, 250 mL Milli-Q water was filled into a double-walled reaction vessel which was connected to a high precision thermostat. The added water was purged with nitrogen for an hour at 80 °C. After an hour, 69 mL of purged water was taken out from the reaction vessel and was stored under nitrogen until further use. Calculated amount of NIPAm (1,71 g) and BA (77,4 mg) monomers were measured into a vial and was purged with nitrogen for 15 min before it was dissolved in 6 mL of oxygen-free water (monomer stock solution I.). APS (0.28 g/10 mL) and SDBS (0.46 g/10 mL) stock solutions were prepared in the same manner. Additionally, a second monomer stock solution was prepared in the same manner, but in this case 10 mol% of the NIPAm monomer was replaced by acrylic acid (monomer stock solution II.). All the stock solutions were stored under nitrogen until use. First, 5 mL of monomer stock solution I. was added to the reaction vessel and was additionally purged with nitrogen for 30 min. This was followed by the addition of calculated amount of SDBS stock solution (2 mL) into the reaction vessel. The reaction mixture was additionally purged for 10 min. The reaction was started by the addition of calculated amount (2 mL) of APS stock solution. The reaction mixture was stirred by a magnetic stirrer at 1500 rpm for 30 s after the initiation. Then the stirring speed was decreased to 500 rpm. After 40 min (~98% conversion), the stirring speed was raised to 1500 rpm and 5 mL of the acrylic acid-containing monomer stock solution (monomer stock solution II.) was added to reaction mixture. The reaction was continued for 4 h. The pNIPAm-shell-pNIPAm-co-10%AAc latex microgel particles were purified from unreacted monomers and surfactant by extensive dialysis against Milli-Q water for 4 weeks giving supernatant conductivity of less than 5 μS/cm. pNIPAm-co-10%AAc-shell-pNIPAm core-shell microgel particles were prepared with the same procedure, but in that case the core monomer solution contained 10 mol% acrylic acid and the addition time of monomer stock solution II. (NIPAm + BA) was chosen to be 29 min (~90% conversion).

2.4. Dynamic light scattering measurements

The dynamic light scattering measurements were performed by means of a Brookhaven dynamic light scattering equipment consisting of a BI-200SM goniometer and a BI-CrossCor cross correlation digital autocorrelator. A Coherent Genesis MX488-1000 STM monomodal laser emitting vertically polarized light was used as light source at a wavelength of 488 nm. The signal analyser was used in the real-time "multi-τ" mode. The time axis is logarithmically spaced over a time interval ranging from 1 μs to 0.1 s. The correlator used 218 time channels. The pinhole was 100 μm. The measurements were performed at a 90° scattering angle. Prior to the measurements, the microgel samples were cleaned of dust by filtering through a 0.8 μm pore-size membrane filter. The intensity-intensity time-correlation functions were measured and then converted to the normalized electric field autocorrelation functions by means of the Siegert relation. The autocorrelation functions were analysed by the cumulant expansion and CONTIN methods. All the samples proved to be practically monodisperse with a polydispersity factor around 1.03.

2.5. Electrophoretic mobility measurements

Malvern Zetasizer Nano ZSP instrument from Malvern Instruments was used to measure the electrophoretic mobility of the pNIPAm microgels as a function of temperature. The instrument uses a combination of laser Doppler velocimetry and phase analysis light scattering (PALS) in a technique called M3-PALS [18]. All measurements were done in 1 mM NaCl as background electrolyte. A total of ten runs were conducted for each measurement. Prior to each series, the instrument was always tested with Malvern zeta-potential transfer standard.

2.6. Monomer conversion measurements

To follow the conversion of the monomers during the synthesis 3 mL samples were taken from the reaction vessel regularly. The samples were taken with a syringe filled with 3 mL of 10 mmol/dm^3 solution of hydroquinone monomethyl ether to ensure immediate inhibition of the polymerization reaction. The unreacted monomers were separated from the polymer by centrifugal filters (Amicon Ultra-4 centrifugal filter devices containing regenerated cellulose membranes with 3 kDa molecular weight cut off; the filter membranes were purified from wetting agents by repeated centrifugation of Milli-Q water). Centrifugation was done by Hettich 220R centrifuge at 6000 rpm and 25 °C. To avoid any dilution of the samples by the water filling the dead volume of the filter units remaining after their purification, the 6 mL samples were centrifuged in three 2 mL portions and only the filtrate of the last sample was collected for further analysis. The filtered samples were analysed by HPLC-UV.

The HPLC system consisted of a Jasco UV-2070 Plus Intelligent UV/VIS detector operating at a wavelength of 224 nm. A Jasco PU-4180 RHPLC one-head pump was used at a flow rate of 1 mL/min. The samples were injected with Model RheoDyne 7125 sample injector equipped with a 25 μl sample loop. All the samples were separated on a Supelco Analytical Discovery HS C18 (10 cm × 4.6 mm; 5 μm) reverse phase column.

Two different eluents were used depending on the composition of the kinetic samples. In the case of pNIPAm homopolymer microgel particles a mixture of 30 V/V% of methanol (VWR Int., HPLC grade) and 70 V/V% of Milli-Q water was used as eluent. In the case of pNIPAm-co-AAc copolymer microgel particles a mixture of 20 V/V% of ethanol (VWR Int., HPLC grade) and 80 V/V% of Milli-Q water was used, whose pH was set to pH 2 by orto-phosphoric acid/sodium dihydrogen phosphate buffer system (the ionic strength of the mixture was set to 100 mmol/dm^3). The eluent was filtered through 1 μm glass filter and degassed in vacuum prior to use. All chromatograms were evaluated with Data Apex Clarity software package.

3. Theoretical background

3.1. Surface charge model of a non-draining colloid particle

According to the classical theory of electrophoretic mobility of colloid particles, the steady state motion of charged, spherical, non-draining particles in an electric field (E) can be described by taking into account that the electric force is balanced by the friction force exerted on the surface of the particle by the liquid. If the thickness of the ionic atmosphere around the particle is negligible compared to the particle size the equality of the forces can be written as:

$$Q_k inE - 6\pi\eta a v_e = 0, \quad (1)$$

where Q_{kin} is sum of all charges present on the particle surface (electrokinetic charge), a is the radius of the particle, η is the viscosity of the medium and v_e is the particle velocity relative to the liquid (electrophoretic velocity). Eq. (1) is the simplest approximation to the electrophoretic velocity of a charged particle. When the ionic atmosphere around the

Please cite this article as: I. Varga, A. Kardos, A. Borsos, et al., Effect of internal charge distribution on the electrophoretic mobility of poly(N-isopropylacrylamide..., Journal of Molecular Liquids, https://doi.org/10.1016/j.molliq.2019.111979

particle is too thick it introduces a correction to Eq. (1) called the electrophoretic retardation force. The applied field acts not only on the charges present on the particle surface but also on the oppositely charged small ions present in the diffuse layer. Since these ions move to the opposite direction they cause a liquid flow which slows down the movement of the central charged particle. Taking into account the additional retardation force the electrophoretic velocity can be expressed as:

$$v_e = \frac{Q_k inE}{6\pi\eta} a + \frac{2E}{3\eta}\int_a^\infty \rho r dr, \tag{2}$$

where ρ is the charge density in the double layer. For relatively thin double layer using the Smoluchowski solution the electrophoretic mobility ($u_e = v_e/E$) of the particle can be expressed as:

$$u_e = \frac{Q_k in}{4\pi\eta\kappa a^2}\left(1+\frac{1}{\kappa a}\right)^{-1}, \tag{3a}$$

$$u_e = \frac{Q_{kin}}{4\pi\eta\kappa a^2}, \quad \text{if } \kappa a \gg 1, \tag{3b}$$

where κ^{-1} is Debey length (the thickness of the double layer) [19].

3.2. Electrophoretic mobility of draining polyelectrolytes

The electrophoretic mobility of liquid-swollen charged colloid particles has initiated several investigations. These particles may contain charges distributed within their liquid swollen internal structure, which can contribute to the electrophoretic mobility of the particles. Ohshima has proposed a general theoretical framework that successfully combined the electrophoretic theories of spherical hard particles and polyelectrolytes [4]. He treated the electrophoretic mobility of spherical soft particles that have a rigid core of radius a, coated by a polyelectrolyte layer with thickness d. To describe the frictional force acting on a particle he adopted the model of Debey and Bueche [20] that is the polymer segments were considered as resistance centres of radius a_p which are uniformly distributed within the polyelectrolyte layer at a volume number density N_p. This permeable porous layer exerts an overall frictional force ($-\gamma \boldsymbol{u}$) on the liquid flow ($\boldsymbol{u}$), where γ is the frictional coefficient of the polyelectrolyte layer. The frictional coefficient is related to the generally used drag coefficient (λ) via the expression:

$$\lambda = \left(\frac{\gamma}{\eta}\right)^{1/2}, \tag{4}$$

where η is viscosity of the liquid. λ^{-1} is also called the electrophoretic softness of the particle, which is the characteristic distance required for the flow to reduce from its value at the particle surface to the value characteristic within a thick polyelectrolyte layer. The general mobility expression derived by Ohshima assumes that the charge distribution of the polyelectrolyte layer has a spherical symmetry and the electric potential is low enough, so the linearized Poisson-Boltzmann equation can be used. Practically this means that the theory neglects any polarization effect. Several limiting cases of the general mobility expressions have been presented from which the following cases are used in the literature to interpret the experimental mobility data of microgel particles.

3.2.1. Spherical polyelectrolyte

In the case of vanishing particle core $a \to 0$ the particle becomes a spherical polyelectrolyte (a porous, permeable, charged sphere of uniformly distributed resistance centres). The exact form of the mobility expression is determined by the charge distribution within the particle. If it is assumed that the polyelectrolyte particle is uniformly charged the following mobility expression can be derived:

$$u_e = \frac{\rho_f ix}{\eta\lambda^2}\left[1+\frac{1\lambda^2}{3\kappa}1+e^{-2\kappa}b-\frac{1-e^{-2\kappa}b}{\kappa b} + \frac{1\lambda^2}{3\kappa}\frac{1+1/\kappa b}{\lambda/\kappa^2-1}\left\{\frac{\lambda}{\kappa}\frac{1+e^{-2\kappa}b-1-e^{-2\kappa}b/\kappa b}{1+e^{-2\lambda}b/1-e^{-2\lambda}b-1/\lambda b}-1-e^{-2\kappa}b\right\}\right], \tag{5}$$

where b is the radius of the spherical polyelectrolyte and ρ_{fix} is its uniform charge density. However, if all charges are accumulated at the surface of the particle providing a uniform surface charge density (σ_{fix}) for the permeable particle the resulting mobility expression is [8]:

$$u_e = \frac{\sigma_f ix}{\eta\lambda}\left[\frac{3}{b}+\frac{8\pi}{b}1-\frac{\lambda b}{3}\frac{\sinh[\lambda b]}{\cosh[\lambda b]-[\sinh\lambda b]/\lambda b}+\frac{8\pi b\lambda^2}{31+\kappa b}\right]. \tag{6}$$

3.2.2. Large diameter particles with thick polyelectrolyte shell

In this case the mobility expression is based on the observation that the potential within the polyelectrolyte layer can be approximated by the Donnan potential if $\kappa a \gg 1$, $\lambda a \gg 1$ as well as $\kappa d \gg 1$ and $\lambda d \gg 1$ hold and the polyelectrolyte layer has a uniform charge density (ρ_{fix}) [4,21]. The model yields the following mobility expression:

$$u_e = \frac{\varepsilon_r\varepsilon_0\psi_0/\kappa_m + \psi_{DON}/\lambda}{\eta\quad 1/\kappa_m} + 1/\lambda + \frac{\rho_{fix}}{\eta\lambda^2}, \tag{7}$$

where ε_r is the relative permittivity of the solution, ε_o is the permittivity of a vacuum, Ψ_{DON} is the Donnan potential in the polyelectrolyte layer, Ψ_o is the potential at the boundary between the polyelectrolyte layer and the solution and κ_m is the effective Debye–Hückel parameter of the polyelectrolyte layer that involves the contribution of the polyelectrolyte charges:

$$\psi_{DON} = \frac{kT}{ze}\ln\left[\frac{\rho_{fix}}{2zen^\infty}+\left\{\left[\frac{\rho_{fix}}{2zen^\infty}\right]^2+1\right\}^{1/2}\right], \tag{7a}$$

$$\psi_0 = \frac{kT}{ze}\ln\left[\frac{\rho_{fix}}{2zen^\infty}+\left\{\left[\frac{\rho_{fix}}{2zen^\infty}\right]^2+1\right\}^{1/2}\right]+\frac{2zen^\infty}{\rho_{fix}}\left[1-\left\{\left[\frac{\rho_{fix}}{2zen^\infty}\right]^2+1\right\}^{1/2}\right], \tag{7b}$$

$$\kappa_m = \kappa\left[1+\left[\frac{\rho_{fix}}{2zen^\infty}\right]^2\right]^{1/4}. \tag{7c}$$

In the above equations k is the Boltzmann constant, T is the absolute temperature, e is the elementary charge, z is the valency of a symmetrical electrolyte present in n^∞ concentration in the bulk phase.

In our calculations the temperature dependence of the permittivity was taken from Lide [22], while the data by Bingham and Jackson [23] were used to calculate the temperature dependence of the viscosity.

4. Results and discussion

To investigate the effect of internal charge distribution on the electrophoretic mobility of soft particles, we prepared pNIPAm microgels with four different internal charge distributions: 1. 'uncharged' microgel particles (N), 2. uniformly charged microgels (C), and core/shell microgels 3. with uncharged core and uniformly charged shell (N–C) and 4. with uniformly charged core and uncharged shell (C–N). The 'uncharged' microgel particles as well as the uniformly charged microgel particles were prepared by the classical batch precipitation polymerization method [14]. In the first case *N*-isopropylacrylamide (NIPAm) monomers were copolymerized with *N,N′*-methylenebis(acrylamide)

Please cite this article as: I. Varga, A. Kardos, A. Borsos, et al., Effect of internal charge distribution on the electrophoretic mobility of poly(N-isopropylacrylamide..., Journal of Molecular Liquids, https://doi.org/10.1016/j.molliq.2019.111979

(BA, 4,31 wt%), while in the latter case the reaction mixture also contained 10% acrylic acid (AAc) monomer. To investigate if the AAc monomers are incorporated uniformly into the growing polymer network, samples were taken regularly from the reaction mixture. The progress of the polymerization reaction was followed by measuring the monomer concentrations in the reaction mixture by HPLC as a function of reaction time. The results of these measurements are shown in Fig. 1a. As it can be seen in the figure the monomer concentrations sharply decrease with increasing reaction time. In agreement with previous results it is also clearly shown that the concentration of BA decreases faster than the concentration of NIPAm giving rise to the formation of a highly crosslinked microgel core. At the same time the concentration of the AAc varies practically parallel with the concentration of NIPAm, which means that the carboxylic groups are distributed uniformly within the polymer network.

In order to synthesize the core shell microgel particles a semi-batch polymerization method was used. In this case the reaction mixture containing the monomers of the particle core was initiated and when most of the monomers have already reacted the monomers of the particle shell were added to the reaction mixture. Since the locus of the polymerization is on the surface of the growing microgel particle [1,15], the particle growth occurs from inside to outside, thus the radial composition of the growing outer shell of the microgel particles can be controlled by the composition of the reaction mixture [16,17,24]. The progress of these polymerization reactions was also followed by measuring the monomer concentrations in the reaction mixture by HPLC as a function of reaction time. The results of these measurements are shown in Fig. 1b and c. As it is shown in the figure the monomers added to the reaction mixture to form the microgel shell reacted on a similar timescale as the monomers of the particle core. Furthermore, it is also indicated that the polymerization rates of NIPAm and AAc are practically identical, implying the formation of uniformly charged particle core or shell. At the same time, it should be noted that when the microgel particles with charged core and 'uncharged' shell were prepared the monomers of the 'uncharged shell' were added when ~10% of the AAc was still in the reaction mixture. This means that in this case AAc was also copolymerized into the microgel shell but in an order magnitude smaller concentration than into the particle core.

The presented kinetic data clearly indicate that the polymerization was successfully performed in each case. To provide evidence for the formation of the desired internal microgel structures, we measured the temperature dependent swelling of the prepared microgel particles in a slightly basic (pH = 9) solution without adding an inert electrolyte. Under these conditions all carboxylic groups were dissociated (charged) and the system had a minimum ionic strength to maximize the swelling of the microgel particles. The results are plotted in Fig. 2. As it is indicated by the figure the four different types of microgel showed dramatically different temperature dependent swelling. The uncharged microgel particles (N) exhibited the typical swelling behavior of pNIPAm [1] showing a volume phase transition ~35 °C. At the same time the uniformly charged microgel particles (C) showed much larger swelling at room temperature and remained in their swollen state in the entire investigated temperature range owing to the presence of the large amount of carboxylic groups (~10% AAc) incorporated uniformly into the polymer network. Due to the dissociation of these carboxylic groups the polymer network becomes charged and remains swollen in the entire investigated temperature range in its total volume. The swelling of the core/shell microgels showed a transition behavior between the uncharged and uniformly charged microgels and showed the typical behavior of core-shell microgels [25]. The room temperature swelling of the charged core/neutral shell microgel (C–N) is significantly larger than the swelling of the uncharged microgel indicating the presence of the charges in the polymer network. The collapse temperature of the 'uncharged' shell is also increased, which is not surprising taking into account that this shell also contains ~1% copolymerized AAc. It is also interesting to note that the final particle size in the

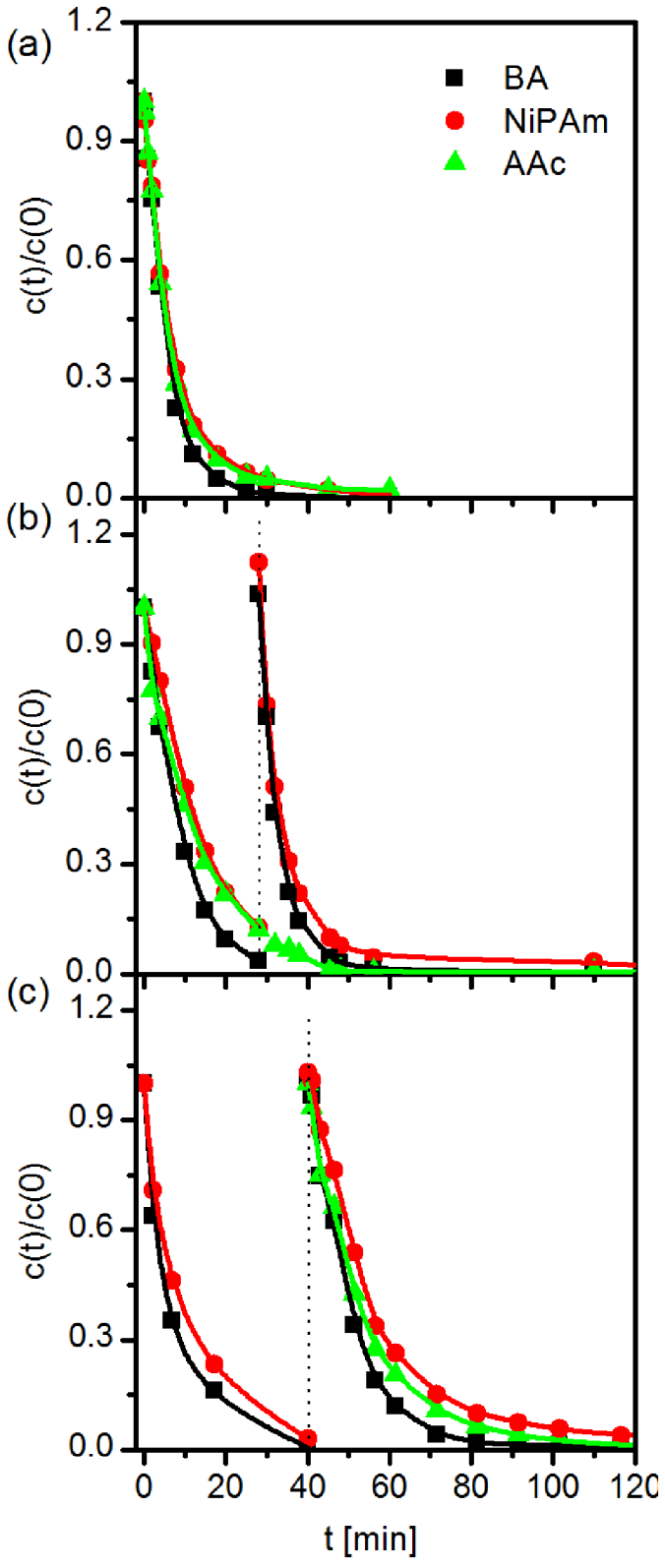

Fig. 1. Relative concentration of the unreacted monomers (NIPAm – red sphere, BA – black square, AAc – green triangle) plotted as a function of reaction time (normalized by their initial concentration in the reaction mixture): (a) homogeneously charged, (b) charged core/uncharged shell, (c) uncharged core/charged shell pNIPAm microgel synthesis. The solid lines are only guide to the eyes. The dotted lines indicate when the monomers of particle shell were given to the reaction mixture. The errors of the data points are commensurate to the size of the symbols in Panels (a), (b) and (c) and not plotted. (For interpretation of the references to colour in this figure legend, the reader is referred to the Web version of this article.)

Please cite this article as: I. Varga, A. Kardos, A. Borsos, et al., Effect of internal charge distribution on the electrophoretic mobility of poly(N-isopropylacrylamide..., Journal of Molecular Liquids, https://doi.org/10.1016/j.molliq.2019.111979

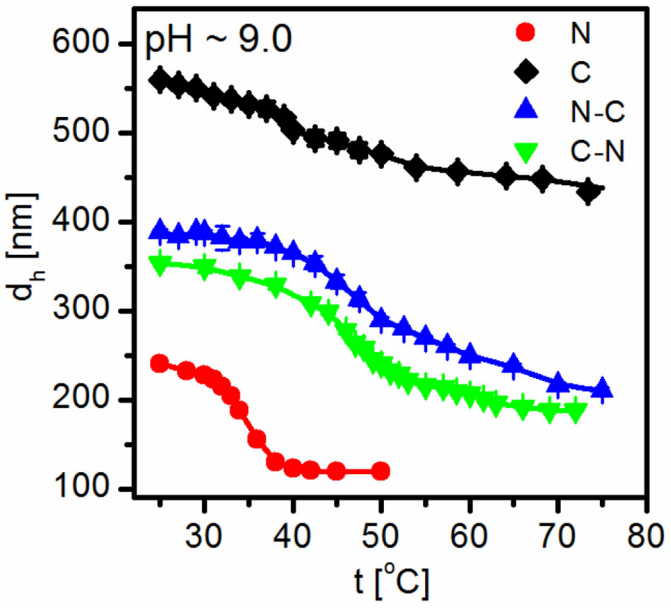

Fig. 2. The hydrodynamic size of the fully charged microgel particles as a function of temperature measured in a slightly basic solution (pH ~ 9) in the absence of inert electrolyte. The acronyms indicate the following microgel electric structure: N – uncharged (neutral), C – uniformly charged, N–C – neutral core with charged shell, C–N – charged core with neutral shell. The lines are only guide to the eyes.

investigated temperature range is much larger than the size of the collapsed pNIPAm microgel indicating that the core of the particles remains in swollen state. The microgel particles prepared with uncharged core and charged shell (N–C) showed larger swelling than the other core/shell microgel. This can be rationalized by taking into account that in this case the loosely crosslinked but highly charged outer shell can swell in a larger extent than the charged core surrounded by a highly crosslinked uncharged shell. To summarize, we can conclude that the swelling characteristics of the prepared microgel particles confirmed the formation of the expected electric structure of the synthetized microgels.

Since the electrophoretic mobility of the microgel particles is strongly dependent on the ionic strength of the medium we performed all of our further measurements in 1 mM NaCl solutions to ensure a constant ionic strength. Furthermore, the pH of all samples was set to 7 to guarantee the dissociation of all carboxylic groups in the polymer network without affecting the ionic strength of the medium. The electrophoretic mobility and the hydrodynamic size of the microgel particles were measured as a function of temperature (pH = 7, I = 1 mM) and the results are plotted in Fig. 3. It is interesting to note that in agreement with the literature the 'neutral' pNIPAm particles also have an electrophoretic mobility because they contain charges originating from the initiator [3,15].

At room temperature the mobility of the uniformly charged (C) and charged shell (N–C) microgel particles is practically the same with significantly higher negative value than that of the 'uncharged' microgel (N). The mobility of the charged core – uncharged shell (C–N) microgel is between the mobility values of the neural core – charged shell (N–C) and neutral particles. Since the core/shell particles have practically identical size (see Fig. 3a), furthermore they contain similar amount but differently localized charges, this observation implies that when the charges are localized in the core of the gel particle they contribute to the electrophoretic mobility in a smaller extent than the charges in the shell. The mobility increases with increasing temperature in all cases due to the decreasing size of the particles.

To gain a better insight how the charges distributed within the microgel particles contribute to the electrophoretic mobility of the microgels first we used the non-draining hard sphere model (Eq. (3)) to evaluate the experimental mobility data of the microgels. If this model is strictly valid then due to the non-draining (hard sphere) nature of the microgel particles only the surface localized charges contribute to the electrokinetic charge, which should remain constant regardless of microgel swelling. Since Eq. (3) allows the unambiguous calculation of the electrokinetic charge of the microgels from the available experimental data, as a first step we determined the electrokinetic charge predicted by this model in the function of the microgel swelling. To highlight the relative changes of the predicted charge, the calculated values are normalized by the charge calculated at 50 °C for each type of microgel. The results are plotted in Fig. 4.

In the case of the 'uncharged' microgel particles (N) the calculated electrokinetic charge does not show any systematic changes with increasing microgel size, which is in agreement with the physical model assumption of a non-draining hard sphere with charges localized on its surface. The calculated electrokinetic charge corresponds to ~600 charged groups on the particle surface, which is ~50% of the number of charges found by titration on similar type of microgel particles

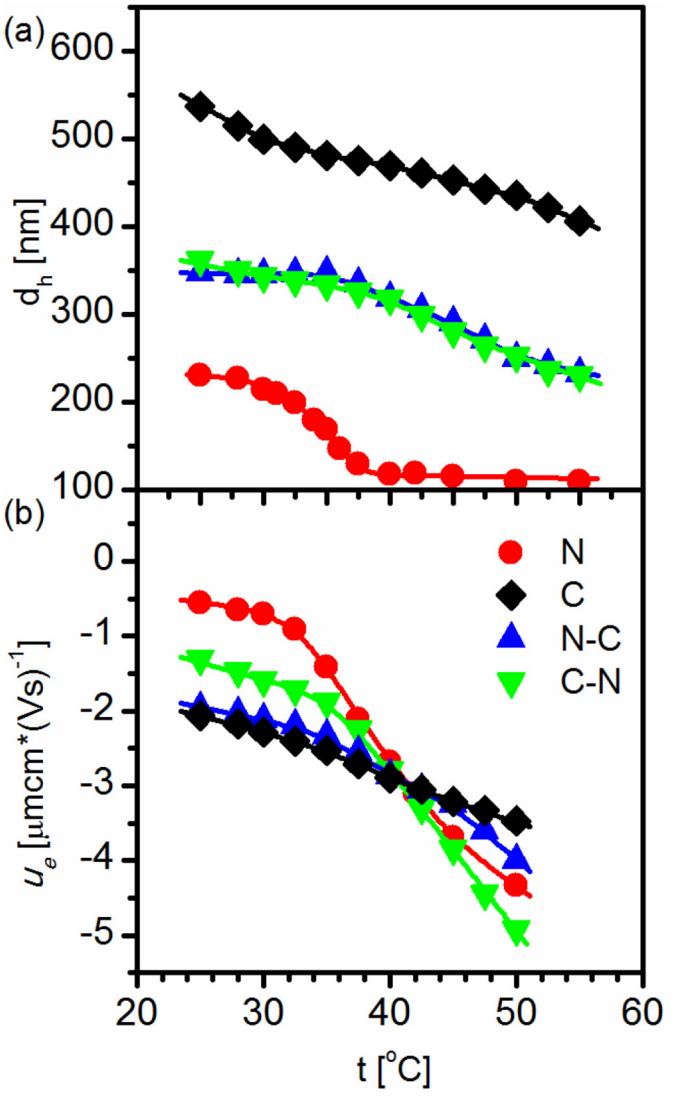

Fig. 3. (a) The hydrodynamic size and (b) the electrophoretic mobility of the microgel particles as a function of temperature at pH = 7.0 in 1 mM NaCl solution. The acronyms indicate the following microgel electric structure: N – uniform uncharged, C – uniform charged, N–C – neutral core with charged shell, C–N – charged core with neutral shell. The lines are only guide to the eyes. The errors of the data points are commensurate to the size of the symbols in Panel (a) and not plotted. Furthermore, the errors of the data points in Panel (b) were found to be around u_e ±0.15 μmcm/Vs but for the clarity of the figure are not plotted.

Please cite this article as: I. Varga, A. Kardos, A. Borsos, et al., Effect of internal charge distribution on the electrophoretic mobility of poly(N-isopropylacrylamide..., Journal of Molecular Liquids, https://doi.org/10.1016/j.molliq.2019.111979

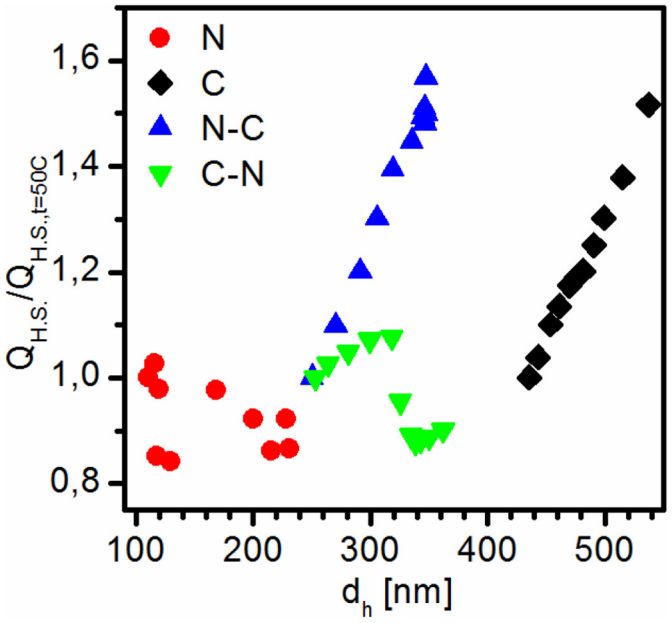

Fig. 4. The electrokinetic charge of the microgel particles given by the non-darning hard sphere model and normalized by the value calculated at t = 50 °C in the function of particle swelling. The acronyms indicate the following microgel electric structure: N – uniform uncharged, C – uniform charged, N–C – neutral core with charged shell, C–N – charged core with neutral shell.

[6,26]. However, this observation is consistent with the non-draining character of the particle, because some of the charges can be localized in the non-draining core of the microgel without contributing to the electrophoretic mobility.

In the case of the homogeneously charged microgel (C) and the core/shell microgel with homogeneously charged shell (N–C), the charged hard-sphere model indicates similarly increasing surface charge with increasing microgel swelling. This observation implies that as the microgels swell new charges are 'generated' on the particle surface. This can be interpreted within the framework of the charged hard sphere model if we assume that the particle 'surface' is a finite thickness surface layer of the microgel particle, whose thickness varies with varying microgel swelling. In this case with increasing microgel swelling we can expect that the thickness of the surface layer increases and more charges can contribute to the electrokinetic charge of the microgel particle, while the inner part of the microgel still behaves as a non-draining hard sphere. At the same time the electrokinetic charge does not level off with increasing swelling even in the case of the most swollen core/shell microgel, which indicates that the thickness of the surface layer remains smaller than the thickness of the outer charged shell of the core/shell microgel.

Finally, we should note that the electrokinetic charge of the microgel particles prepared with a charged core and uncharged shell (C–N) show only a small non-monotonous variation with particle swelling. These variations are also consistent with the physical picture that with increasing swelling the particle core remains non-draining and only a thin surface layer contribute to the electrokinetic charge. The small initial increase of the electrokinetic charge can be explained by the increasing thickness of this surface layer. However, as it was explained previously in this case the charge density of the external 'neutral' shell of the microgel is an order of magnitude smaller than in the case of the microgels with charged outer shell (C and N–C), which explains that only a moderate increase of the electrokinetic charge is indicated with increasing swelling by the model. At the same time at an intermediate swelling the calculated electrokinetic charge suddenly drops to a smaller value than the initial charge at 50 °C. To interpret this result, we have to remember that the pNIPAm microgel particles are not uniformly crosslinked but there are less crosslinked dangling chains both on the outer surface if the charged core and on the uncharged shell. Furthermore, at high temperature the outer uncharged shell is in a collapsed state. This may allow some of the outer dangling chains of the charged core to reach the surface layer that provides the surface charge. With decreasing temperature, the outer uncharged shell may swell beyond the range where the dangling charged chains of the particle core can reach, thus the charge density of the outer shell drops with the swelling of the uncharged shell as it is indicated by the results.

To summarize by assuming that the surface charges of practically non-draining microgel particles are localized in a surface layer that has a varying thickness with varying microgel swelling the experimental electrophoretic behavior of the microgel particles prepared with different internal charge distributions can be interpreted physically consistently in terms of the charged hard sphere model. However, as it has already been demonstrated in the literature, both the hard sphere model (Eq. (3)) and the draining polyelectrolyte models (Eqs. (4)–(6)) can be fitted to the experimental mobility data of the microgels. Thus, as a next step we also wanted to test if the draining models could provide a physically consistent interpretation of our experimental results. However, as it is indicated by Eqs. (4)–(6), the electrophoretic mobility of a draining particle is dependent on the internal charge distribution of the particle. Since in the case of the prepared core/shell particles we cannot derive reliable radial charge density distribution functions as a function of microgel swelling our analysis on the electrophoretic mobility of the draining particles is restricted to the homogeneously charged and 'uncharged' microgels.

The electrophoretic mobility of the draining microgel beads is constrained by two limiting cases. One of them is the free draining limit of the gel beads. In the free-draining limit the polymer segments present in a gel particle are regarded as independent resistance centres of radius a_s distributed uniformly within the gel bead at a segment density N_s. It is assumed that the hydrodynamic interaction of the polymer segments can be neglected, thus each segment contributes the same Stokes resistance to the frictional coefficient (γ) of the microgel bead [4]:

$$\gamma = 6\pi\eta a_s N_s. \tag{8}$$

The free draining limit is expected to be valid while the density of the polymer segments is low within the draining particle (high porosity). However, if the segment concentration increases hydrodynamic interactions develop, the flow slows down within the particle and the segments in the particle core experience smaller drag force than the ones close to the particle surface. The other limiting case is the non-draining limit when there is no flow through the gel bead due to the strong hydrodynamic interactions. The water present inside the microgel particle moves together with the gel bead, thus the inner polymer segments does not experience the drag force. This means that in this case only the surface segments contribute to the friction coefficient. As it is implied by the above summary the level of draining through the microgel particles has a profound effect on the drag force and thus on the electrophoretic mobility. Though, Ohshima's model provides a formal description of this effect with some limitation, it does not provide any guidance on the level of hydrodynamic interactions. Thus, in literature investigations the drag coefficient (λ) is usually described in terms of the polymer chain density either by using Brinkman's model [27], or empirical expressions [8,28].

However, taking into account that the total charge of a gel bead (Q_{gel}) is a physically invariant characteristic of the microgel particle regardless of its swelling, instead of using a priory assumption about the swelling dependence of the drag coefficient (λ), it can be determined directly from experimental data and analysed. Namely, if the charges are localized at the surface of, or distributed uniformly within a draining particle, then the surface charge density (σ_{fix} in Eq. (6)) or the volume charge density (ρ_{fix} in Eq. (5)) can be expressed in terms of the

Please cite this article as: I. Varga, A. Kardos, A. Borsos, et al., Effect of internal charge distribution on the electrophoretic mobility of poly(N-isopropylacrylamide..., Journal of Molecular Liquids, https://doi.org/10.1016/j.molliq.2019.111979

analytical charge (Q_{gel}) and the hydrodynamic radius ($R_h \approx b$) of the particle:

$$\sigma_{fix} = \frac{Q_{gel}}{4\pi {R_h}^2} \text{ or } \rho_{fix} = \frac{3Q_{gel}}{4\pi {R_h}^3}, \tag{9}$$

Substituting these expressions into Eqs. (5) and (6), the drag coefficient (λ) acting on the gel particle can be determined once the electrophoretic mobility (u_e), the hydrodynamic size ($R_h \approx b$) and the analytical charge (Q_{gel}) of the gel beads have been determined.

To facilitate the analysis of the electrophoretic data in terms of the draining models we determined the analytical charge of the 'neutral' and the homogeneously charged microgel particles. We used potentiometric titrations to determine the charge of the microgel particles, which were found 3.8 μeq/g and 805 μeq/g, respectively. In previous investigations the microgel molar mass was found to be in the range of 2–5x10^8 g/mol [29]. Using these values as lower and upper limits we converted the titration results into the charge of the individual microgel particles. The results are plotted in Fig. 5a where the estimated range of particle charge is plotted as a light blue and a light-yellow band for the 'uncharged' pNIPAm and the homogeneously charged pNIPAm-co-10% AAc microgels, respectively.

As a next step we also calculated an upper and a lower limit of the electrokinetic charge of the microgel particles based on the experimental mobility data. Since the charges of the 'uncharged' pNIPAm microgel particles are originating from the persulfate initiator, which tend to accumulate at the particle surface the surface charged particle model (Eq. (6)) was used to calculate their electrokinetic charge. At the same time in the case of homogeneously charged pNIPAm-co-10%AAc microgels the kinetic measurements indicated that the AAc monomers are incorporated uniformly in the polymer network, so in this case the homogeneously charged particle model was used (Eq. (5)). The lower limit of the electrokinetic charge of the draining particles was determined by assuming that the microgel particles behave as free draining particles. The drag coefficients of the free draining particles were estimated using Eqs. (4) and (8). To ensure that the calculated values represent a lower limit for the electrokinetic charge the radius of the resistance centres (a_s) was given as 1 nm, while the segment density in the gel beads (N_s) was calculated from the monomer density ($N_{Mon} = n_{Mon}/V_{MG}$, where n_{Mon} is the number of monomers in the V_{MG} volume of the microgel particle) by overestimating the number of monomers forming a polymer segment (100 monomers/segment). It should be noted that the choice of these parameter values had only a small effect on the calculated free draining limit of the electrokinetic charge and did not affect our conclusions. The upper limit of the electrokinetic charge of the draining particles is represented by the non-draining limit of the model, which is characterized by a diverging drag coefficient ($\lambda \to \infty$). It is straightforward to show that in this case Eq. (5) reduces to (assuming that $R_h = b$):

$$u_e = \frac{\rho_{fix}}{3\eta\kappa^2}\left(1 + e^{-2\kappa}R_h - \frac{1-e^{-2\kappa}R_h}{\kappa R_h}\right), \tag{10a}$$

$$u_e = \frac{\rho_{fix}}{3\eta\kappa^2} = \frac{Q_{gel}}{4\pi\eta}(\kappa R_h)^2 R_h, \quad \text{if } \kappa R_h \gg 1 \tag{10b}$$

for the homogeneously charged particles, while Eq. (6) reduces to:

$$u_e = \frac{\sigma_{fix}}{\eta}\frac{8\pi R_h}{3(1+\kappa R_h)}, \tag{11a}$$

$$u_e = \frac{8\pi}{3\eta\kappa}\sigma_{fix} = \frac{2Q_{gel}}{3\eta\kappa {R_h}^2}, \quad \text{if } \kappa R_h \gg 1 \tag{11b}$$

for the charged surface particles.

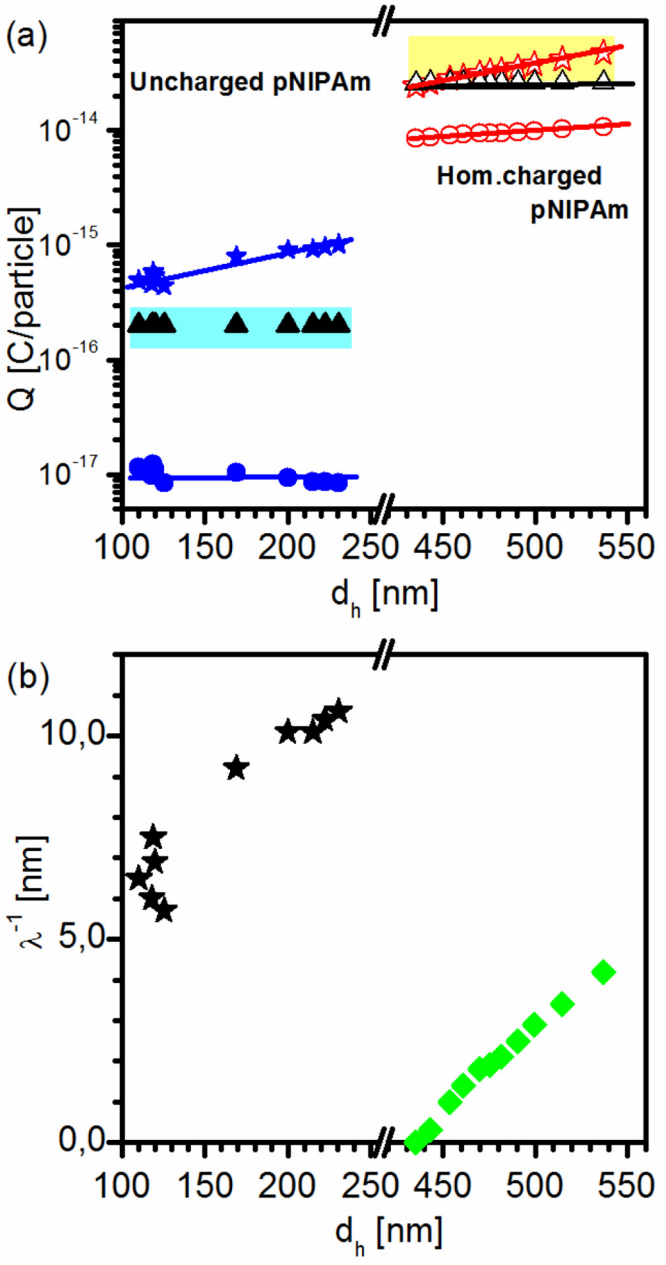

Fig. 5. (a) The electrokinetic charge of the 'uncharged' (solid blue symbols) and the homogeneously charged (open red symbols) microgels determined from experimental electrophoretic mobility values in the free-draining limit (spheres) and in the non-draining limit (stars) of draining particle model. The electrokinetic charge used to fit the electrophoretic softness of the microgels is plotted by black solid triangles for the uncharged pNIPAm and by black open triangles for the charged ones. The physically realistic range of the microgel analytical charge estimated from titration is plotted as light blue and light-yellow bands for the 'uncharged' and for the homogeneously charged microgels, respectively. (b) The electrophoretic softness fitted for the 'uncharged' microgel (black stars) and for the homogeneously charged microgels (green diamonds). (For interpretation of the references to colour in this figure legend, the reader is referred to the Web version of this article.)

The calculated lower and upper limits of the electrokinetic charge values are also plotted in Fig. 5a for both the 'uncharged' (solid blue symbols) and for the homogeneously charged microgels (open red symbols). In the case of the 'uncharged' microgel particles the analytical charge of the microgel particles determined from titration is within the limits of the electrokinetic charge determined from the mobility values. Practically this means that the constant (electrokinetic/analytical) charge of the draining particle can be ensured by fitting the drag coefficient in Eq. (6), while keeping the electrokinetic charge of the

Please cite this article as: I. Varga, A. Kardos, A. Borsos, et al., Effect of internal charge distribution on the electrophoretic mobility of poly(N-isopropylacrylamide..., Journal of Molecular Liquids, https://doi.org/10.1016/j.molliq.2019.111979

microgel particle fixed in the entire range of microgel swelling. To determine how the drag coefficient of pNIPAm particle varies with particle swelling we have fixed the electrokinetic charge value in the middle of the range expected from the titration (2×10^{-16} C/particle). The reciprocal values of the fitted drag coefficients (the electrophoretic softness values – λ^{-1}) are plotted in Fig. 5b. As it could be expected the fitted electrophoretic softness value increases with microgel swelling and the fitted values are in good agreement with previous results.

In the case of the homogeneously charge pNIPAm-co-10%AAc microgel particles the physically realistic analytical charge range (light-yellow region in Fig. 5a) indicated by the titration coincides with the upper limit of the electrokinetic charge determined by the experimental electrophoretic mobility values (open red stars in Fig. 5a). This means that a physically realistic constant microgel charge that falls within the range allowed by the titration but remains lower than the upper limit determined from the electrophoretic value must be limited for the lower limit allowed by the titration (open black triangle). We used this value (2.6×10^{-14} C/particle) to determine the drag coefficient of pNIPAm-co-10%AAc microgel particles in the investigated range of particle swelling. The determined electrophoretic softness data (λ^{-1}) are also plotted in Fig. 5b (green diamonds). Though, with increasing swelling the softness of the microgel particles again increases, the electrophoretic softness of the charged microgel is found significantly smaller than the values fitted for the 'uncharged' particles. Taking into account that the charged microgels are highly swollen in the investigated temperature range, while the 'uncharged microgel' is fully collapsed at high temperatures these results seem to contradict to the physical model that the level of draining (the electrophoretic softness) is related to the segment density within the particle. It should also be noted that the highly swollen state of the charged microgel at the highest investigated temperature has another implication: with further temperature increase the microgel can further shrink and consequently its electrophoretic softness should also further decrease. However, according to Fig. 5b this is not possible since the electrophoretic softness has already reached its minimum value, which is an evident physical inconsistency. In principle this inconsistency could be resolved if the homogeneously charged microgel particles have a smaller molecular weight than we used as a lower limit in our estimation of the microgel charge, thus the microgel charge would be smaller and the corresponding softness higher. However, taking into account that the homogeneously charged microgel particles have a larger collapsed size at pH = 3 than the collapsed size of the 'uncharged' microgels used to determine the microgel molecular weight [29] this does not seem a physically solid explanation. To summarize we can conclude that though the parameters of the draining models can be fitted to the experimental mobility values measured for the investigated microgels, the results seem to be physically inconsistent for the different microgel particles and with the model assumptions.

To rationalize our results, it should be highlighted that recently new scaling arguments have been presented in the literature to interpret the molecular weight independence of the thermophoretic mobility of high molecular weight polymers [12,13]. It is a well-established fact that when the molecular weight of a polymer becomes large enough its thermal diffusion coefficient becomes molecular weight independent. This is often interpreted as the proof of the free-draining character of the polymer coil during thermal diffusion. The presented model however demonstrated that with increasing segment number the hydrodynamic interactions within the polymer coil diverge and the polymer coil becomes non-draining in a thermophoretic experiment. It was also shown that this leads to the experimentally observed molecular weight independence of the thermophoretic mobility. Since in the case of an electrophoretic mobility experiment the draining characteristics of the microgels also play an outstanding role, here we adopt the presented arguments to gain a better insight into the effect of hydrodynamic interactions on the electrophoretic mobility of the microgel particles.

Now, let us consider a microgel particle immersed into a dilute electrolyte solution. Let us assume that the microgel particle is built up by N_s polymer segments and each of them has the same Q_s charge compensated by monovalent mobile ions (M). When the microgel particle is exposed to an electric field ($\boldsymbol{E}$) it experiences a driving force ($\boldsymbol{f_{MG}}$), which causes the relative motion of the microgel particle to the liquid phase with a velocity $\boldsymbol{v_{MG}} = \mu_{MG}\boldsymbol{f_{MG}}$, where μ_{MG} is the mobility of the microgel particle, which can be related to the diffusion coefficient of the microgel (D_{MS}) by the Stokes-Einstein relationship, $\mu_{MG} = D_{MS}/k_BT$. Furthermore, since the polymer segments are connected with each other the total driving force acting on the gel network is equally shared among the polymer segments, thus $\boldsymbol{f_{MG}} = N_s{}^*\,\boldsymbol{f_s}$, where $\boldsymbol{f_s}$ is the force on each segment. If hydrodynamic interactions were not present, then the water molecules and the small ions present in the solution could flow freely within the microgel particle and the microgel could move with a velocity characteristic for the individual segments. However, the moving segments drag liquid with themselves that produces a hydrodynamic drag force ($\boldsymbol{f_h}$) on each segment and small ion within the microgel particle. Let us consider a spherical monovalent small ion (M) with radius a_M within the microgel particle. As a first approximation the force on this small ion ($\boldsymbol{f_M}$) can be calculated as the sum of the electric force originating from its interaction with the external electric field ($\boldsymbol{f_{E,M}}$) and the hydrodynamic drag force induced by the moving microgel segments ($\boldsymbol{f_{h,M}}$). The movement of the small ion will be determined by the relative magnitude of these forces: when $\boldsymbol{f_{E,M}} \gg \boldsymbol{f_{h,M}}$, then the small ion can move freely and practically does not experience the effect of the polymer segments (free draining); however, if $\boldsymbol{f_{h,M}} \gg \boldsymbol{f_{E,M}}$, then the ion is dragged with the microgel particle. The total hydrodynamic force exerted by the moving polymer network on a small ion within the microgel particle can be expressed as follows [12,13]:

$$\boldsymbol{f}_{\mathbf{h,M}} = 6\pi\eta a_M \langle \textstyle\sum_j \boldsymbol{u}_{\mathbf{j}}\mathbf{r}_{\mathbf{Mj}} \rangle = \mu_M^{-1} \langle \textstyle\sum_j \boldsymbol{u}_{\mathbf{j}}\mathbf{r}_{\mathbf{Mj}} \rangle \tag{12}$$

where a_M is the small ion radius, $\boldsymbol{u_j}$ is the flow field around segment j, $\boldsymbol{r_{Mj}}$ is the distance of segment j from the small ion M, $<>$ is the average over polymer configurations and μ_M is the mobility of the small ion. As it was shown by Yang et al.:

$$\langle \textstyle\sum_j \boldsymbol{u}_{\mathbf{j}}\mathbf{r}_{\mathbf{Mj}} \rangle = -\frac{N_s}{6\pi\eta} R_h, MG^{-1}\boldsymbol{f_s} = N_s a_s \mu_s R_h, MG^{-1}\boldsymbol{f_s}, \tag{13}$$

where $R_{h,MG}$ is the hydrodynamic radius of the microgel and μ_s is the mobility of a microgel segment. Substituting Eq. (13) into Eq. (12):

$$\boldsymbol{f}_{\mathbf{h,M}} = \mu_M^{-1} N_s a_s \mu_s R_h, MG^{-1}\boldsymbol{f_s}. \tag{14}$$

Taking into account that all segment in the microgel particle move with the same average speed ($\boldsymbol{v_s}$), which is equal to the speed of the moving microgel particle ($\boldsymbol{v_{MG}}$):

$$\mu_s \boldsymbol{f_s} = \boldsymbol{v_s} = \boldsymbol{v_{MG}} = u_e, MG\boldsymbol{E}, \tag{15}$$

$$\boldsymbol{f}_{\mathbf{h,M}} = \mu_M^{-1} N_s a_s u_e, MG\boldsymbol{E} R_h, MG^{-1}, \tag{16}$$

where $u_{e,MG}$ is the electrophoretic mobility of the microgel and $\boldsymbol{E}$ is the external electric field.

To express the electric force acting on the small ion ($\boldsymbol{f_{E,M}}$) we should remember that the velocity of the small ion can be expressed either as $v_e, M = u_e, ME$, or as $v_e, M = \mu_M f_E, M$, which gives rise to:

$$\boldsymbol{f}_{\mathbf{E,M}} = \mu_M^{-1} u_e, M\boldsymbol{E}. \tag{17}$$

Please cite this article as: I. Varga, A. Kardos, A. Borsos, et al., Effect of internal charge distribution on the electrophoretic mobility of poly(N-isopropylacrylamide..., Journal of Molecular Liquids, https://doi.org/10.1016/j.molliq.2019.111979

Taking the ratio of the driving force values acting on the small ion (M), we get:

$$\frac{f_{h,M}}{f_{E,M}} \sim \frac{u_{e,MG}}{u_{e,M}} \frac{N_s a_s}{R_{h,MG}} \sim \frac{N_s a_s}{R_{h,MG}}, \tag{18}$$

since the electrophoretic mobility of the small ion ($u_{e,M}$) and the microgel ($u_{e,MG}$) is the same order of magnitude and do not scale with N_s. To interpret Eq. (18), we have to take into account that a microgel particle is a chemically crosslinked polymer network, which is built up by $n_{ch} \gg 1$ pieces of sub-chains connected by the cross-links. For the sake of simplicity we may assume that each polymer sub-chain contains $N_{s,ch}$ segments between two cross-links, thus the number of polymer segments within the microgel can be written as $N_s = n_{ch}{}^* N_{s,ch}$, while the volume of the microgel can be expressed as $V \sim R_h^3 \sim n_c h R_s, ch^3$, where $R_s, ch \sim a_s N_s, ch^{\nu}$, is the hydrodynamic radius of a sub-chain, where the exponent ν is ~3/5 in a good solvent, ½ in Θ solution and 1/3 in a bad solvent.

$$\frac{f_h, M}{f_E, M} \sim n_{ch}^{2/3} \cdot N_{s,ch}^{1-\nu} \gg 1, \tag{19}$$

since both $n_{ch} \gg 1$ and $N_{s,ch} \gg 1$.

What Eq. (19) tells is that the hydrodynamic force dominates within the microgel particle, thus the relative motion of the small ions is prevented compared to the polymer network, they are dragged with the microgel particle. In other words, the microgel core is non-draining, and the flow lines are pushed out of the particle inner core to its surface layer. This also means that if $\kappa^{-1} \ll R_h$ any volume element within the microgel core must be electro-neutral. Combining the non-draining character of the particle core and its electroneutrality, we can conclude that the charges present in the microgel core do not contribute to its electrophoretic mobility.

Between the non-draining core and the external fluid there must be a transition layer. As it has been shown the thickness of this layer (L) is inversely proportional to the square root of the segment density within the polymer ($L \sim n_s^{-1/2}$) [30]. This means that its actual magnitude is strongly affected by the swelling of the microgel particle, which in turn depends on the cross-link density of the gel ($N_{s,ch}$), and the swelling of the sub-chains ($R_s, ch \sim a_s N_s, ch^{\nu}$) that is affected by e.g. the temperature, pH and ionic strength. Altogether, as the particle swelling increases (the segment density decreases) the transition layer becomes thicker and as a consequence more charges contribute to the electrophoretic mobility of the microgel. However, it is straightforward to show that the thickness of this layer will be small compared to the size of the microgel particle even if the microgel is in its swollen state ($\nu = 3/5$):

$$\frac{L}{R_{h,MG}} \sim \frac{n_s{}^{-1/2}}{R_{h,MG}} \sim \left(\frac{N_{s,ch}}{R_{s,ch}^3}\right)^{-1/2} \frac{1}{R_{h,MG}} \sim a_s^{1/2} n_{ch}^{-1/3} \cdot N_{s,ch}^{(\nu-1)/2} \ll 1. \tag{20}$$

To summarize we can conclude that the above arguments reveal that the microgel particles behave as compact colloid (non-draining) particles regardless of their swelling state and only the charges present in a thin surface layer contribute to the electrophoretic driving force. At the same time with increasing swelling the thickness of this layer increases facilitating the increase of the electrokinetic charge when the charges are distributed in the outer shell of the microgel. These arguments are in very good agreement with experimental mobility data we determined for microgel particles with four different internal charge distributions in the function of the microgel swelling.

5. Conclusions

In this work we prepared four different pNIPAm-based microgel particles with different internal electric structures and measured their electrophoretic mobility and hydrodynamic size as a function of microgel swelling. Our data show that though the draining particle models can be used to fit the experimental electrophoretic mobility data and to determine the electrophoretic softness of the microgel particles, the fitted parameter values are not coherent with the physical model assumptions when the results gained for an 'uncharged' and for a homogenously charged microgel are compared. At the same time when it is assumed that the microgel particles have a non-draining core and a thin draining shell whose thickness increases with particle swelling, the experimental data are in good agreement with the model predictions.

To rationalize these observations, we also presented scaling arguments to show that the hydrodynamic drag force acting on the small ions in the core of a microgel particle far exceeds the electrophoretic driving force. As a consequence, the core of the gel particle becomes non-draining and it is expected that the counterions of the charged network present in this non-draining core are dragged with the microgel particle and the particle core behaves as a neutral hard core in an electrophoretic experiment. The electrophoretic charge of the microgels is provided by a thin draining shell, whose thickness increases with particle swelling.

Declarations of interest

None.

Acknowledgments

Attila Kardos gratefully acknowledges that this work supported by the New National Excellence Program of the Ministry of Human Capacities, Hungary, ÚNKP-18-3. This research has also received funding from the People Programme (Marie Curie Actions) of the European Union's Seventh Framework Programme, European Commission, FP7/2007–2013/under REA GA290251, from the Hungarian National Research, Development and Innovation Office (NKFIH), Hungary, K116629 and from the Ministry of Human Capacities, Hungary, (1783-3/2018/FEKUTSRAT), which is gratefully acknowledged. This publication is the partial result of the Research & Development Operational Programme for the project "Modernization and Improvement of Technical Infrastructure for Research and Development of J. Selye University in the Fields of Nanotechnology and Intelligent Space", Slovakia, ITMS 26210120042 and the operation program called Research and Innovation for the project: "Support of research and development capacities in the area of nanochemical and supramolecular systems" , code ITMS2014+ 313011T583, funded from the resources of the European Regional Development Fund.

Appendix A. Supplementary data

Supplementary data to this article can be found online at https://doi.org/10.1016/j.molliq.2019.111979.

References

[1] R.H. Pelton, Temperature-sensitive aqueous microgels, Adv. Colloid Interface Sci. 85 (2000) 1–33, https://doi.org/10.1016/S0001-8686(99)00023-8.
[2] T. Hoare, R. Pelton, Functional group distributions in carboxylic acid containing poly (N-isopropylacrylamide) microgels, Langmuir 20 (2004) 2123–2133, https://doi.org/10.1021/la0351562.
[3] R.H. Pelton, H.M. Pelton, A. Morphesis, R.L. Rowell, Particle sizes and electrophoretic mobilities of poly(N-isopropylacrylamide) latex, Langmuir 5 (1989) 816–818, https://doi.org/10.1021/la00087a040.
[4] H. Ohshima, Electrophoresis of soft particles, Adv. Colloid Interface Sci. 62 (1995) 189–235, https://doi.org/10.1016/0001-8686(95)00279-Y.

[5] H. Ohshima, K. Makino, T. Kato, K. Fujimoto, T. Kondo, H. Kawaguchi, Electrophoretic mobility of latex particles covered with temperature-sensitive hydrogel layers, J. Colloid Interface Sci. 159 (1993) 512–514, https://doi.org/10.1006/jcis.1993.1356.
[6] T. Gilányi, I. Varga, R. Mészáros, G. Filipcsei, M. Zrínyi, Characterisation of monodisperse poly(*N*-isopropylacrylamide) microgel particles, Phys. Chem. Chem. Phys. 2 (2000) 1973–1977, https://doi.org/10.1039/B000571L.
[7] L. Nabzar, D. Duracher, A. Elaıssari, G. Chauveteau, C. Pichot, Electrokinetic properties and colloidal stability of cationic amino-containing *N*-Isopropylacrylamide −Styrene copolymer particles bearing different shell structures, Langmuir 14 (1998) 5062–5069, https://doi.org/10.1021/la980244l.
[8] A. Fernández-Nieves, A. Fernández-Barbero, F.J. de las Nieves, B. Vincent, Motion of microgel particles under an external electric field, J. Phys. Condens. Matter 12 (2000) 3605–3614, https://doi.org/10.1088/0953-8984/12/15/309.
[9] A. Fernández-Nieves, M. Márquez, Electrophoresis of ionic microgel particles: from charged hard spheres to polyelectrolyte-like behavior, J. Chem. Phys. 122 (2005) https://doi.org/10.1063/1.1844392084702-084702-6.
[10] T. Gilányi, I. Varga, R. Mészáros, G. Filipcsei, M. Zrínyi, Interaction of monodisperse poly(*N*-isopropylacrylamide) microgel particles with sodium dodecyl sulfate in aqueous solution, Langmuir 17 (2001) 4764–4769, https://doi.org/10.1021/la0100800.
[11] T. Hoare, R. Pelton, Electrophoresis of functionalized microgels: morphological insights, Polymer 46 (2005) 1139–1150, https://doi.org/10.1016/j.polymer.2004.11.055.
[12] K.I. Morozov, W. Köhler, Thermophoresis of polymers: nondraining vs draining coil, Langmuir 30 (2014) 6571–6576, https://doi.org/10.1021/la501695n.
[13] M. Yang, M. Ripoll, Driving forces and polymer hydrodynamics in the Soret effect, J. Phys. Condens. Matter 24 (2012) 195101, https://doi.org/10.1088/0953-8984/24/19/195101.
[14] X. Wu, R.H. Pelton, A.E. Hamielec, D.R. Woods, W. McPhee, The kinetics of poly(*N*-isopropylacrylamide) microgel latex formation, Colloid Polym. Sci. 272 (1994) 467–477, https://doi.org/10.1007/BF00659460.
[15] A. Kardos, T. Gilányi, I. Varga, How small can poly(N-isopropylacrylamide) nanogels be prepared by controlling the size with surfactant? J. Colloid Interface Sci. 557 (2019) 793–806, https://doi.org/10.1016/j.jcis.2019.09.053.
[16] I. Antoniuk, D. Kaczmarek, A. Kardos, I. Varga, C. Amiel, Supramolecular hydrogel based on pNIPAm microgels connected via host–guest interactions, Polymers 10 (2018) 566, https://doi.org/10.3390/polym10060566.
[17] A. Kardos, I. Varga, Preparation of poly(N-isopropylacrylamide) microgel beads with double hydrophilic shells in a single pot reaction. – Unpublished results.
[18] Malvern Instrument Ltd., Zeta Sizer Nano Z User Manual, Worcestershire, WR14 1XZ, United Kingdom, 2004.
[19] D. Stigter, in: H.K. van Olphen, Mysels J. Theorex, La Jolla (Eds.),Enriching Topics from Colloid and Surface Science 1975, pp. 293–307.
[20] P. Debye, A. Bueche, Intrinsic viscosity, diffusion, and sedimentation rate of polymers in solution, J. Chem. Phys. 16 (1948) 573, https://doi.org/10.1063/1.1746948.
[21] H. Ohshima, Theory of electrostatics and electrokinetics of soft particles, Sci. Technol. Adv. Mater. 10 (2009), 063001. https://doi.org/10.1088/1468-6996/10/6/063001.
[22] D.R. Lide, Handbook of Chemistry and Physics, 78th ed. CRC Press, New York, 1997 1998.
[23] E.C. Bingham, R.F. Jackson, Bull. Bur. Stds. 14 (1918) 75.
[24] R. Acciaro, T. Gilanyi, I. Varga, Preparation of monodisperse poly(N-isopropylacrylamide) microgel particles with homogenous crosslink density distribution, Langmuir 27 (2011) 7917–7925, https://doi.org/10.1021/la2010387.
[25] J. Kleinen, A. Klee, W. Richtering, Influence of architecture on the interaction of negatively charged multisensitive poly(*N*-isopropylacrylamide)-co-Methacrylic acid microgels with oppositely charged polyelectrolyte: absorption vs adsorption, Langmuir 26 (2010) 11258–11265, https://doi.org/10.1021/la100579b.
[26] W. McPhee, K.C. Tam, R. Pelton, Poly(N-isopropylacrylamide) latices prepared with sodium dodecyl sulfate, J. Colloid Interface Sci. 156 (1993) 24–30, https://doi.org/10.1006/jcis.1993.1075.
[27] H.C. Brinkman, Problems of fluid flow through swarms of particles and through macromolecules in solution, Researcher 2 (1949) 190–194.
[28] P.C. Carman, Fluid flow though granular beds, Trans. Inst. Chem. Eng. 15 (1937) 150–166.
[29] I. Varga, T. Gilányi, R. Mészáros, G. Filipcsei, M. Zrínyi, Effect of cross-link density on the internal structure of poly(N-isopropylacrylamide) microgels, J. Phys. Chem. B 105 (2001) 9071–9076, https://doi.org/10.1021/jp004600w.
[30] A.Y. Grosberg, A.R. Khokhlov, Statistical Physics of Macromolecules, American Institute of Physics, New York, 1994.

Please cite this article as: I. Varga, A. Kardos, A. Borsos, et al., Effect of internal charge distribution on the electrophoretic mobility of poly(N-isopropylacrylamide..., Journal of Molecular Liquids, https://doi.org/10.1016/j.molliq.2019.111979